Am J Transl Res 2017;9(11):4807-4820
www.ajtr.org /ISSN:1943-8141/AJTR0058335

Original Article

Tetramethylpyrazine phosphate and borneol combination therapy synergistically attenuated ischemia-reperfusion injury of the hypothalamus and striatum via regulation of apoptosis and autophagy in a rat model

Bin Yu[1,2*], Ming Ruan[3*], Tao Liang[2], Shi-Wen Huang[1], Sheng-Jin Liu[2], Hai-Bo Cheng[1], Xiang-Chun Shen[4]

[1]Jiangsu Engineering Laboratory for Research and Industrialization of Empirical Formulae, Nanjing University of Chinese Medicine, Nanjing 210023, China; [2]Jiangsu Key Laboratory for Pharmacology and Safety Evaluation of Chinese Materia Medica, School of Pharmacy, Nanjing University of Chinese Medicine, Nanjing 210023, China; [3]Jiangsu Provincial Key Construction Laboratory of Special Biomass Waste Resource Utilization, School of Food Science, Nanjing Xiaozhuang University, Nanjing 211117, China; [4]The Key Laboratory of Optimal Utilization of Natural Medicinal Resources, School of Pharmaceutic Science, Guizhou Medical University, Huaxi University Town, Guian New District, Guiyang 550025, China. [*]Equal contributors.

Received May 27, 2017; Accepted October 30, 2017; Epub November 15, 2017; Published November 30, 2017

Abstract: The combination of tetramethylpyrazine (TMP) and borneol (BO) has shown promise for treatment of cerebral ischemia in clinical and experimental studies. However, the mechanism for the synergistic effect of these compounds is unclear. In this study, global cerebral ischemia-reperfusion (GCIR) was induced in rats that were subsequently treated with tetramethylpyrazine phosphate (TMPP) (13.3 mg/kg), BO (0.16 g/kg), or the combination TMPP + BO. Neuronal ultrastructure and intracellular calcium [Ca^{2+}]i levels were evaluated in hypothalamus and striatum. Neuron autophagy was evaluated by expression of LC3 II/I, ULK1, Beclin1, BNIP3, mTOR, and pAMPK. Neuron apoptosis was examined via apoptosis index (AI) and expression of p53, Bcl-2, Bax, and caspase-3. Both monotherapies significantly improved neuronal ultrastructure, reduced numbers of apoptotic neurons and AI, attenuated [Ca^{2+}]i overload, increased expression of pAMPK, ULK1, and LC3 II/I, and markedly reduced expression of mTOR, p53, and caspase-3 in hypothalamus and striatum. In hypothalamus, TMPP increased Bcl-2 expression and decreased Bax expression. In striatum, TMPP and BO increased Beclin1 expression while TMPP increased Bcl-2 expression and decreased Bax expression. TMPP + BO combination therapy enhanced expression of LC3 II/I, pAMPK, mTOR, and ULK1 in hypothalamus, and pAMPK, mTOR, ULK1, Beclin1, and Bax in striatum compared to the monotherapies. Combination therapy synergistically modulated p53 and adjusted Bcl-2 in striatum compared to TMPP and BO monotherapies, respectively. These results demonstrated a synergistic effect of TMPP + BO in protecting against hypothalamus and striatum in rats from ischemia-reperfusion injury and suggested that the mechanism involved shifting neurons from harmful apoptosis to protective autophagy and reducing neuronal [Ca^{2+}]i.

Keywords: Synergistic effect, tetramethylpyrazine phosphate, borneol, apoptosis, autophagy, intracellular calcium content

Introduction

Global cerebral ischemia is a frequent sequela to cardiac arrest, shock, severe hypertension, and brain injuries, and always leads to selective and delayed neuronal death. In addition to neurons of the cortex and hippocampus, the hypothalamus and striatum are brain regions also susceptible to injury [1-4]. It has been confirmed that the ischemia-induced abnormalities in the hypothalamus and striatum lead to adverse systemic effects [5, 6]. Therefore, it is important to seek effective anti-ischemia therapeutic strategies and explore their underlying mechanisms in these two brain regions.

Apoptosis and autophagy play roles in the cerebral injury induced by ischemia. It has been

shown that the process of apoptosis is always accompanied by enhanced expression of Bax, caspase-3, and p53, and reduced expression of Bcl-2. In addition, activation of the caspase family, especially caspase-3, is a crucial event in the caspase-dependent apoptosis pathway [7]. Autophagy, a widespread physiological process in higher eukaryotes, contributes not only to maintaining cellular homeostasis by regulating cell growth and differentiation during the developmental period, but also to adaptation to various metabolic stressors by removal of aggregate-prone proteins and damaged organelles. It has been reported that a certain degree of autophagy is essential for the stabilization of neurons [8].

Tetramethylpyrazine (TMP) is one of the most important active ingredients from *Ligusticum chuanxiong Hort*. (chuan xiong), a traditional Chinese medicinal herb. TMP phosphate (TMPP), as a commercial product, is usually prescribed for patients with cerebral ischemia in the clinic [9]. Protection of the brain from injury due to ischemia involves the reduction of inflammation, NO production, and oxidative stress [10-12]. Borneol (BO), a resin from *Dryobalanops aromatica Gaertn. F.*, has been acknowledged to attenuate Alzheimer's disease, stroke, cerebral ischemia, cerebritis, and cerebral edema in traditional Chinese medicine [13]. We previously demonstrated that BO efficiently crossed the blood-brain-barrier (BBB) and was distributed in the brain [14, 15]. In addition, there is experimental evidence that BO monotherapy attenuates the effects of brain ischemia via its anti-oxidation and anti-inflammation activities [16-18]. Moreover, BO has been shown to enhance the protective effects of TMPP in the cerebrum in numerous clinical and experimental studies [19-22]. Our previous study confirmed the neuroprotection conferred by the two drugs against ischemia-induced injury in the hypothalamus and striatum regions, and showed that TMPP and BO worked synergistically [23]. However, the underlying mechanism of protection of the combination therapy is still unclear.

The current investigation was undertaken to further ascertain the potential targets of TMPP and BO in modulating apoptosis- and autophagy-related signaling pathways in the hypothalamus and striatum in a rat model of cerebral ischemia. In addition, the mechanism of synergy was explored to understand the clinical effects observed.

Experimental procedures

Materials and animals

TMPP and BO were purchased from Livzon Pharmaceutical Group, Inc. (Shaoguan, China) and Nanjing Pharmaceutical Co., Ltd. (Nanjing, China), respectively. Clear grade male Sprague-Dawley rats (250-300 g) were obtained from Shanghai Slac Laboratory Animal Co., Ltd. (Shanghai, China). The rats were housed at the animal facility of Nanjing University of Chinese Medicine with a 12-h light/12-h dark cycle and constant room temperature of 25°C with free access to food and water. The care and use of the rats were approved by the Animal Ethics Committee of Nanjing University of Chinese Medicine and the experiment was performed strictly according to the Guidelines of Laboratory Animal Care and Use (Institute of Laboratory Animal Resources, Commission on Life Sciences, National Research Council, 1996).

Surgical induction of GCIR

Because the four vessels of the bilateral vertebral arteries (VA) and common carotid arteries (CCA) contribute to maintenance of cerebral blood flow and blood oxygen availability, the four-vessel occlusion model was employed to mimic GCIR injury in the clinic; the technique was performed as previously described [23]. Briefly, after rats were anesthetized with chloral hydrate (300 mg/kg, intraperitoneally), the bilateral VA were located using a lens and completely occluded by electrocauterization. Then, the bilateral CCA were wrapped with thread for later occlusion. For CCA occlusion, the rats were anesthetized with 2.5% atomized halothane. The CCA were occluded using an artery clip for 10 min followed by reperfusion for 24 h. Rats that exhibited loss of righting reflex for 60 s, had bilateral dilated pupils, and that lacked a response to light during ischemia were selected for the study. Animals in the sham group were prepared in the same way but without electrocauterization of the vertebral artery and occlusion of the CCA. All surgeries were per-

formed under anesthesia and body temperature was maintained at 37 ± 0.5°C using a thermal blanket during the surgical procedure.

Grouping and drug administration

Sixty-four GCIR rats were randomly divided into four groups: model group, TMPP group, BO group, and the TMPP + BO group. Each group consisted of sixteen rats. Sham and test groups were given physiological saline via intragastric route. The treatment groups received TMPP (13.3 mg/kg), BO (0.16 g/kg), or TMPP + BO (13.3 mg/kg TMPP and 0.16 g/kg BO), respectively. All drugs were given once daily for 7 days. After the treatment period, groups of rats were sacrificed as described below, and brain tissues were harvested and used for the following evaluations.

TUNEL staining

TUNEL (terminal deoxynucleotidyl transferase-mediated dUTP nick end-labeling) analysis was employed to evaluate apoptotic neurons. Rats were deeply anesthetized by chloral hydrate (300 mg/kg, ip.), then perfused with physiological saline followed by 4% paraformaldehyde. After the brains were removed, the hypothalamus and striatum tissues were separated using a brush followed by fixation in 4% paraformaldehyde for 30 days. After being dehydrated in alcohol, the tissues were embedded in paraffin and cut into 5 μm sections. TUNEL staining was performed according to the instructions of the TUNEL assay kit (Roche Diagnostics Corp., Indianapolis, IN). Tissues were evaluated by a researcher who was blinded to the group assignments. The average numbers of TUNEL-positive neurons and the total neurons were calculated from three random visual fields. The apoptosis index (AI) was the ratio of TUNEL-positive neurons to total neurons.

Examination of ultrastructure

Small pieces (< 1 mm^3) of hypothalamus and striatum tissue were excised from the whole brain and fixed in 2% glutaraldehyde (0.1 M phosphate buffer, pH 7.4) for 3 hours, then post-fixed with 1% OsO_4 and 0.8% potassium ferricyanide for 1 h at 4°C. The section was dehydrated in a graded series of acetone, embedded in Epon 812 epoxy resin, and sliced into ultrathin sections. After staining with uranyl acetate and lead citrate, samples were examined using an H7650 transmission electron microscope (Hitachi, Tokyo, Japan).

Laser confocal Ca^{2+} imaging

After the rats were deeply anesthetized and decapitated, the brain was quickly removed and immersed in ice cold DMEM solution, which was filled with 95% O_2 and 5% CO_2. Hypothalamus and striatum were separated. Then the two brain tissues were sliced at 300 μm thickness using a VT1000 S Vibratome (Leica, Germany). After a slice was stabilized on a cover glass in oxygenated DMEM solution for 30 min at room temperature, it was incubated with 5 μM Fluo-3/AM (Biotium, Hayward, CA, USA) for another 30 min, and then washed twice with D-Hank's solution. The fluorescence intensities in hypothalamic and striatal neurons were detected by a laser scanning confocal microscope (Leica TCS-SP5, Solms, Germany). Line scanning mode was used at a scan rate of 1 kHz. The excitation wavelength was 488 nm and emission wavelength was from 505 to 530 nm. The fluorescence intensity reflected the intracellular calcium content.

Western blot assay

Hypothalamus and striatum tissues were separated rapidly on an ice box after harvesting of the rat brain. Cerebral tissue was homogenized in an ice-cold tissue lysis buffer (1 mM EDTA), and 2.5 mL of cell lysate was centrifuged at 16,000 rpm for 10 min at 4°C. The protein concentration in the supernatant was determined by bicinchoninic acid (BCA) protein assay (Nanjing KeyGen Biotech. Co., Ltd., Nanjing, China). The supernatant was diluted to 7 μg/μL with gel loading buffer and heated for 4 min at 95°C. Then, 10 μL (70 μg) of the protein sample was separated by SDS-PAGE and transferred to a polyvinylidine fluoride (PVDF) membrane. The membrane was blocked for 2 h at room temperature in Tris-buffered saline with Tween-20 (TBST) containing 5% bovine serum albumin (BSA), and then was probed with the following primary antibodies overnight at 4°C: anti-LC3 I/II, anti-ULK1 and anti-Beclin1 (1:1000; Cell Signaling Technology, Beverly, MA, USA), anti-BNIP3 (1:1000; Abcam, Cambridge, UK), anti-

Table 1. Accession numbers, primers, and product sizes for real-time PCR assay

Target genes	Accession no.	Forward (5'-3')	Reverse (5'-3')	Size (bp)
Caspase-3	NM_001009338.1	GTGTGCGTTAGAAGTACC	GTTCTTTTGTGAGCATAG ACA	834
Bcl-2	DQ926871.1	GAGATGTCCAGCCAGCTG	TAGGCACCCAGGGTGATG	365
Bax	DQ926869.1	CAGCTCTGAGCAGATCATG	TGGTGGCCTCAGCCCATCT	539
P53	NM_205264.1	GAGTGCTGAAGGAGATCAATGAG	GTGGTCAGTCCGAGCCTTTT	145
GAPDH	NM_017008.4	GTTCAACGGCACAGTCAAG	GCCAGTAGACTCCACGACAT	136

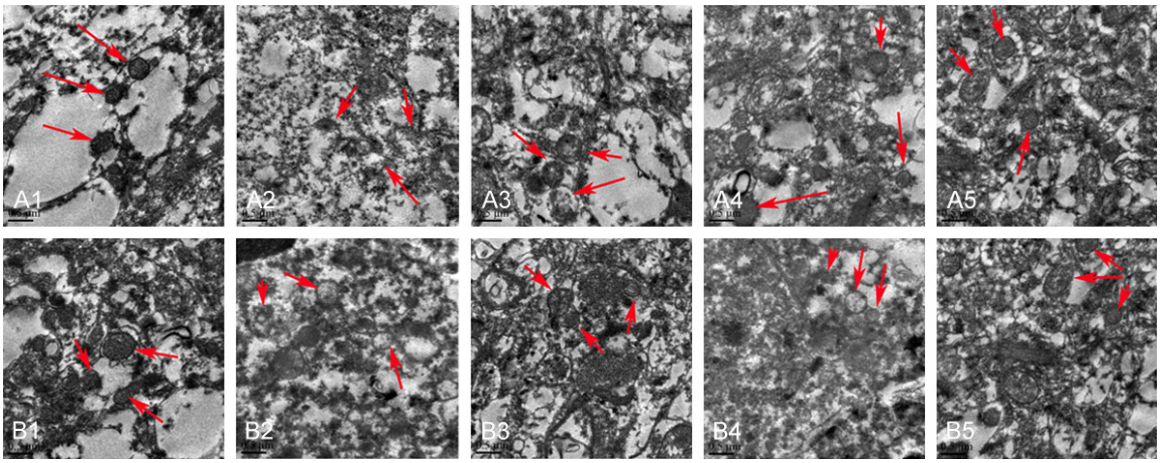

Figure 1. The synergistic effect between TMPP and BO on the ultrastructure of hypothalamus and striatum neurons measured by transmission electron microscopy. (A1-A5) are representative images of neurons in hypothalamus of sham, model, TMPP (13.3 mg/kg), BO (0.16 g/kg), and TMPP (13.3 mg/kg) + BO (0.16 g/kg) groups, respectively. (B1-B5) are representative images of neurons from striatum of sham, model, TMPP, BO, and TMPP + BO groups, respectively. The red arrows denote the mitochondria in neurons of each group. Neurons from the model group showed significant disorganization, including swollen mitochondria and endoplasmic reticulum, lysis of the plasma membrane, and empty vacuoles. Treatment with TMPP, BO, or the combination significantly attenuated these abnormalities caused by ischemic injury, especially regarding the structure of mitochondrial cristae.

mTOR and anti-pAMPK (1:1000; Santa Cruz Biotechnologies, Dallas, TX, USA). Anti-β-actin (1:5000; Bioworld Technology, Inc., St. Louis Park, MN, USA) was used as control for protein gel loading. After washing in TBST, the membrane was incubated for 2 h with secondary antibody (goat anti-rabbit 1:10,000, Boster Biotechnology, Ltd., Wuhan, China). Proteins were detected by enhanced chemiluminescence method, and blots were analyzed using Image-J software. β-actin was used for normalization.

Real-time PCR assay

Hypothalamus and striatum were separated as described above. Total RNA was extracted with Trizol reagent according to the manufacturer's instructions. Then, the total RNA was reverse transcribed using the iScript cDNA Synthesis Kit (Bio-Rad, Hercules, CA, USA). cDNAs for p53, Bcl-2, Bax, caspase-3, and GAPDH were amplified by PCR using the SYBR Premix Ex Taq™ kit (TakaRa Bio Inc., Shiga, Japan) in an MJ Mini thermal cycler (Bio-Rad). Reaction conditions: pre-incubation at 95°C 5 min followed by 40 cycles of 95°C 15 s and 60°C 40 s. Melting curve analysis was performed from 55°C to 95°C. Cycle number threshold (Ct) of each reaction was calculated from the amplification curve using the $2^{-\Delta\Delta Ct}$ method to derive relative gene expression. Accession numbers, primers, and product sizes are shown in **Table 1**.

Statistical analysis

Data were expressed as means ± standard deviation (SD) and analyzed using SPSS13.0 software. Statistical differences among groups

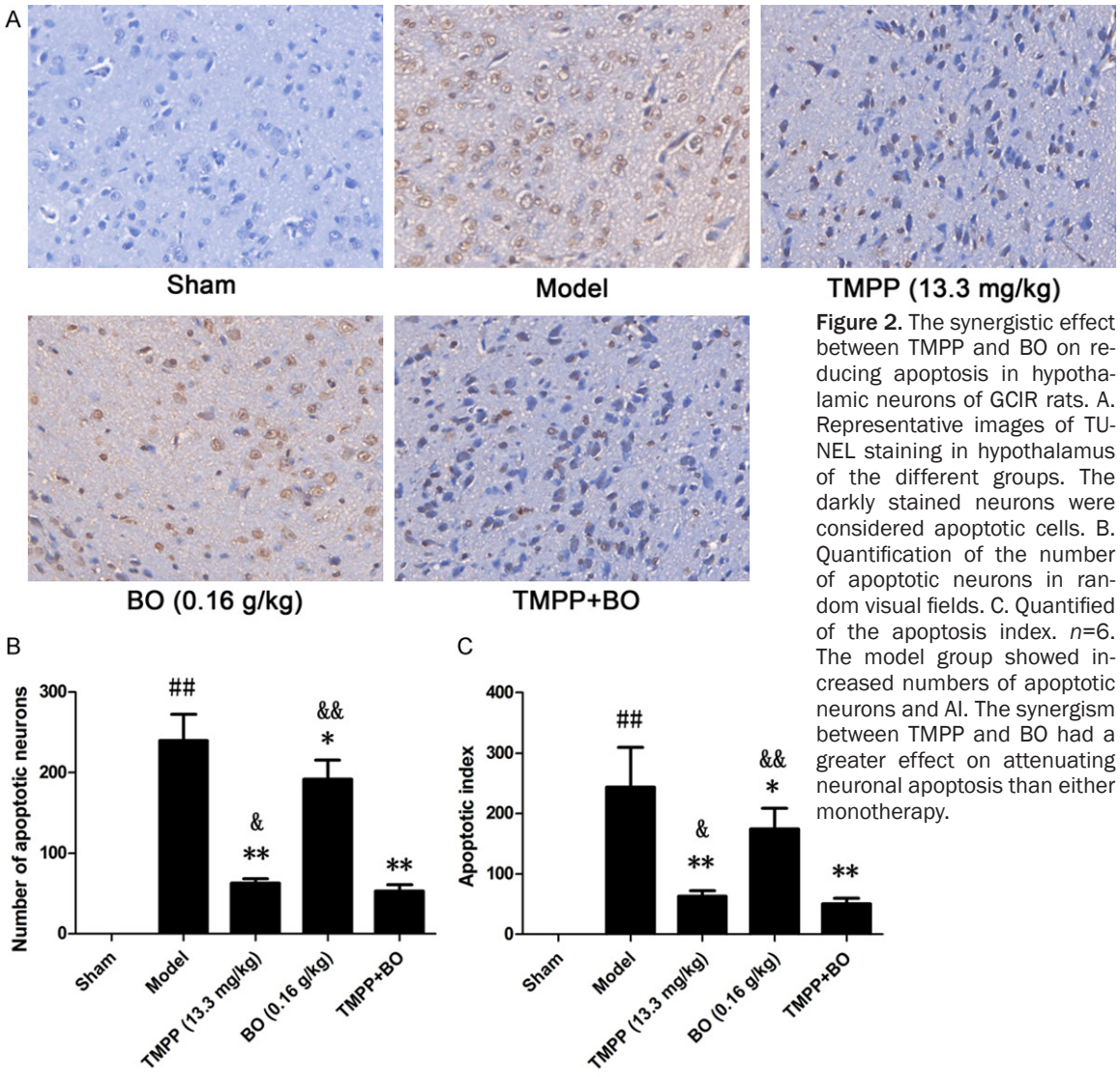

Figure 2. The synergistic effect between TMPP and BO on reducing apoptosis in hypothalamic neurons of GCIR rats. A. Representative images of TUNEL staining in hypothalamus of the different groups. The darkly stained neurons were considered apoptotic cells. B. Quantification of the number of apoptotic neurons in random visual fields. C. Quantified of the apoptosis index. *n*=6. The model group showed increased numbers of apoptotic neurons and AI. The synergism between TMPP and BO had a greater effect on attenuating neuronal apoptosis than either monotherapy.

were analyzed by one-way analysis of variance (ANOVA) and Turkey's multiple comparison post hoc test. A $p < 0.05$ was considered statistically significant.

Results

TMPP + BO combination therapy resulted in improved neuronal ultrastructure in hypothalamus and striatum of GCIR rats

Transmission electron microscopy was used to evaluate the morphologies of organelles, including plasma membrane, mitochondria, endoplasmic reticulum, and nucleus. Compared to the hypothalamus (**Figure 1A1**) and striatum (**Figure 1B1**) of the sham groups, the organelles in both hypothalamic and striatal neurons of the model group showed significant disorganization, including loss of mitochondrial cristae, degeneration of endoplasmic reticulum, lysis of the nuclear membrane, and formation of empty vacuoles (**Figure 1A2**, **1B2**). TMPP, BO, and TMPP + BO treatments significantly attenuated the abnormalities caused by ischemic injury, especially regarding the structure of the mitochondrial cristae in hypothalamic neurons (**Figure 1A3-A5**), as well as striatal neurons (**Figure 1B3-B5**).

TMPP + BO combination therapy resulted in reduced apoptosis of neurons in hypothalamus and striatum of GCIR rats

TUNEL staining was employed to demonstrate whether the neuroprotection by TMPP + BO combination therapy involved regulation of ap-

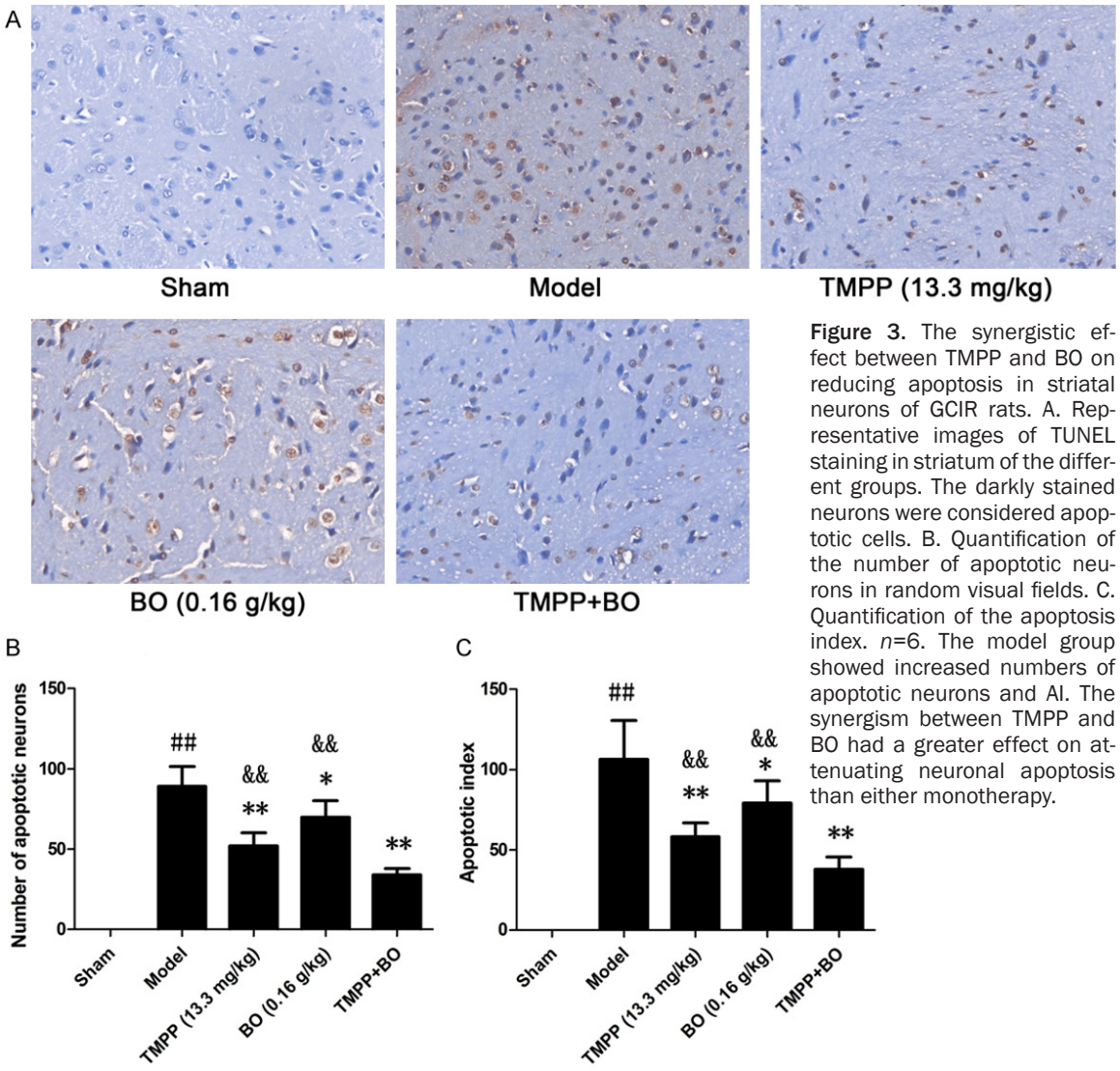

Figure 3. The synergistic effect between TMPP and BO on reducing apoptosis in striatal neurons of GCIR rats. A. Representative images of TUNEL staining in striatum of the different groups. The darkly stained neurons were considered apoptotic cells. B. Quantification of the number of apoptotic neurons in random visual fields. C. Quantification of the apoptosis index. *n*=6. The model group showed increased numbers of apoptotic neurons and AI. The synergism between TMPP and BO had a greater effect on attenuating neuronal apoptosis than either monotherapy.

optosis. Darkly stained neurons were regarded as apoptotic cells in the histomorphological images (**Figures 2**, **3**). Compared with the sham groups, the model group had a marked increase in number of apoptotic neurons and AI ($p < 0.01$). After treatment with TMPP, BO, or the combination, there was a significant reduction in number of apoptotic neurons and AI compared to the model group ($p < 0.05$, $p < 0.01$, respectively). In addition, attenuation of apoptosis was more pronounced in the TMPP + BO combination therapy group compared to either monotherapy group ($p < 0.01$).

Synergistic effect between TMPP and BO in regulating neuronal [Ca^{2+}]i in hypothalamus and striatum of GCIR rats

Figures 4, **5** illustrate the results of intracellular [Ca^{2+}] measurement in neurons of hypothalamus and striatum. Compared to the sham group, the model group had significantly increased [Ca^{2+}]i in neurons from both areas ($p < 0.01$), which suggested Ca^{2+} overload. Treatment with TMPP, BO, or the combination attenuated the increase of [Ca^{2+}]i compared to the model group ($p < 0.05$). Moreover, the TMPP + BO combination resulted in greater attenuation than the TMPP or BO monotherapy group ($p < 0.05$, $P < 0.01$, respectively). These results demonstrated a synergistic effect of TMPP + BO in attenuating [Ca^{2+}]i.

Synergistic effect between TMPP and BO in regulating the expression of the autophagy-related proteins in hypothalamus and striatum of GCIR rats

Figures 6, **7** show the protective autophagy induced by treatment with TMPP, BO, or the

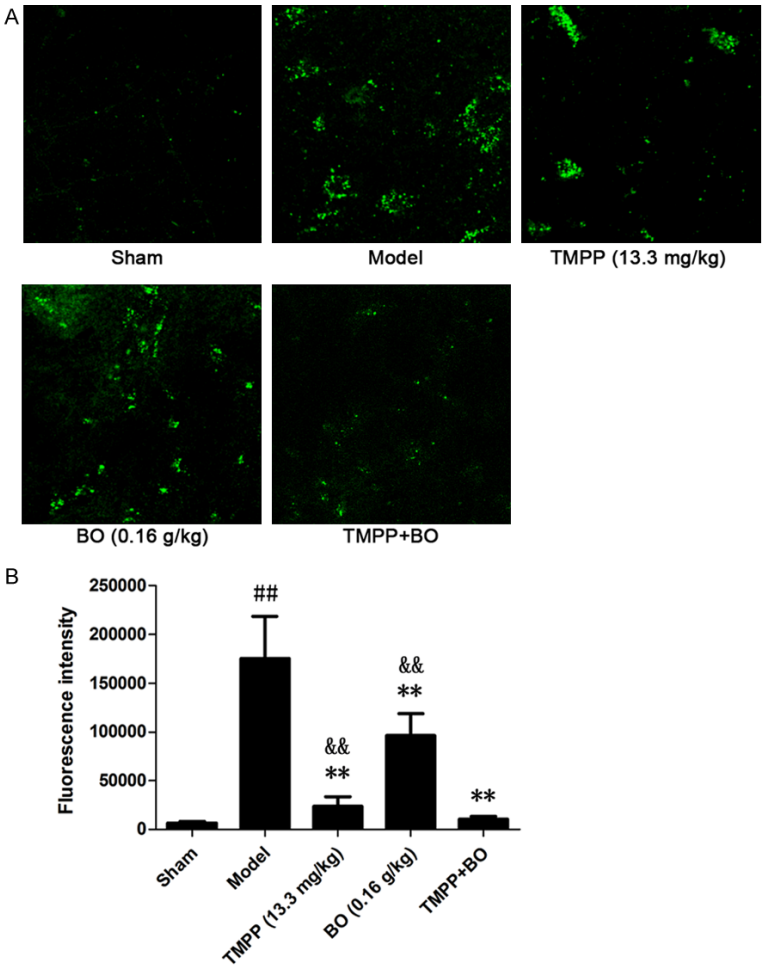

Figure 4. The synergistic effect between TMPP and BO on regulating intracellular calcium concentration in hypothalamic neurons of GCIR rats. (A) are representative laser confocal images of sham, model, TMPP (13.3 mg/kg), BO (0.16 g/kg), and TMPP (13.3 mg/kg) + BO (0.16 g/kg) groups, respectively. (B) Column charts of intracellular calcium concentration in each group. *n*=6. Results for the model group indicated intracellular overload of calcium. Treatment with TMPP, BO, or the combination, significantly attenuated neuronal calcium overload. The effect of the combination therapy was greater than either monotherapy.

combination on GCIR injury in rats. Compared to the sham group, the model rat group had a significant increase in expression of LC II/I, Beclin1, BNIP3, and ULK1 in the hypothalamus and LC II/I, Beclin1, BNIP3, pAMPK, and ULK1 in the striatum ($p < 0.05$, $p < 0.01$, respectively). These changes indicated that autophagy had been triggered by GCIR injury. However, it was interesting that autophagy was not down-regulated, but was up-regulated after treatment with BO, TMPP, or the combination. The regulation of protein expression by these treatments involved different target molecules. In hypothalamus, TMPP and BO increased the expression of pAMPK, ULK1, and LC3 II/I and markedly reduced expression of mTOR ($p < 0.05$, $p < 0.01$, respectively). In striatum, TMPP and BO treatment resulted in similar regulation as observed in hypothalamus, with the exception of increased Beclin1 expression ($p < 0.05$, $p < 0.01$, respectively). In addition, the combination therapy affected the expression of some of the proteins including LC3 II/I, pAMPK, mTOR and ULK1 in hypothalamus, and pAMPK, mTOR and ULK1 in striatum more strongly compared to the TMPP and BO monotherapies ($p < 0.05$, $p < 0.01$, respectively).

Synergistic effect between TMPP and BO in regulating the expression of apoptosis-related genes in hypothalamus and striatum of GCIR rats

As shown in **Figure 8**, expression of p53, Bax, and caspase-3 mRNA was significantly up-regulated and Bcl-2 was down-regulated in the model group compared to the sham group ($p < 0.01$), which suggested that apoptosis had been induced by GCIR damage. Interestingly, the effects of treatment with TMPP, BO, or the combination in hypothalamus were similar to those in striatum. All three treatments resulted in significantly decreased levels of p53 and caspase-3 mRNA in the two brain regions ($p < 0.05$, $p < 0.01$, respectively). Moreover, both TMPP and the combination therapy resulted in increased Bcl-2 and markedly decreased Bax expression ($p < 0.05$, $p < 0.01$, respectively). Although, the combination therapy did not exhibit a curative effect in hypothalamus, it was more effective in modulating p53 and Bax expression compared to the TMPP group, and Bax and Bcl-2 compared to the BO group in striatum ($p < 0.05$, $p < 0.01$, respectively).

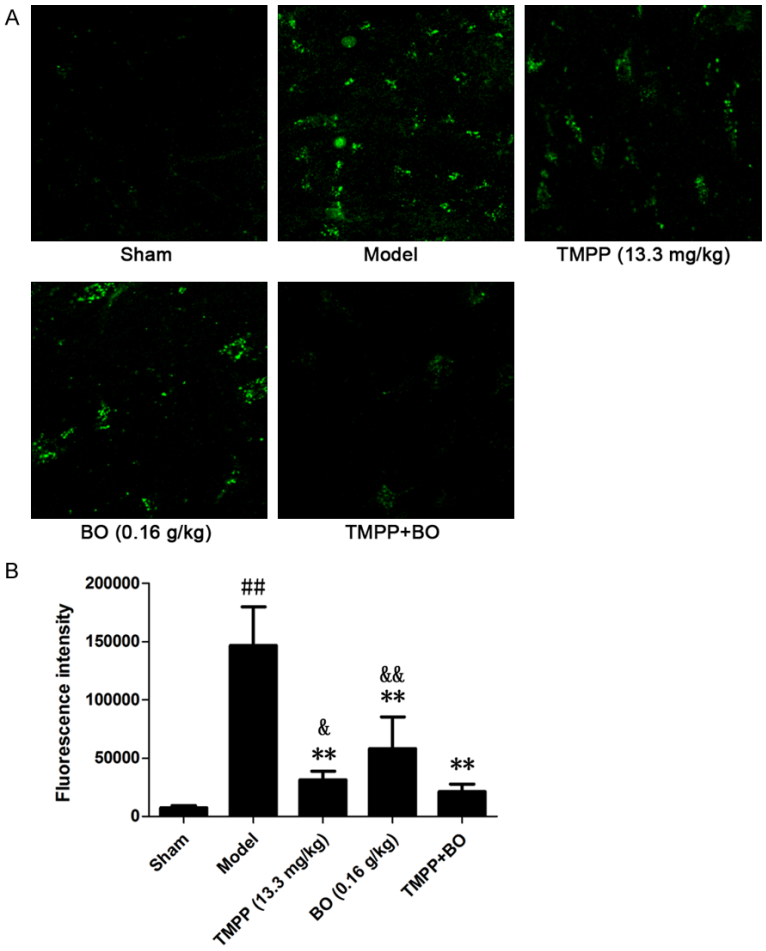

Figure 5. The synergistic effect between TMPP and BO on regulating intracellular calcium concentration in striatal neurons of GCIR rats. (A) are representative laser confocal images of sham, model, TMPP (13.3 mg/kg), BO (0.16 g/kg), and TMPP (13.3 mg/kg) + BO (0.16 g/kg) groups, respectively. (B) Column charts of intracellular calcium concentration in neurons from each group. *n*=6. The model group indicated intracellular overload of calcium. Treatment with TMPP, BO, or the combination, significantly attenuated neuronal calcium overload. The effect of the combination therapy was greater than either monotherapy.

Discussion

In contrast to cortex and hippocampus, hypothalamus and striatum have received much less attention regarding treatment of ischemic injury. However, there has been increasing evidence to suggest that hypothalamic and striatal neurons are as vulnerable to ischemia as cortical and hippocampal neurons [1, 24]. A number of reports demonstrated that ischemia and inflammation of hypothalamus, rather than body hyperthermia, are the main results of heatstroke, which may lead to multi-organ dysfunction syndrome (MODS) [25]. In this study, we examined the synergistic benefit of TMPP + BO combination therapy, and explored the underlying mechanism of brain protection against ischemic injury of hypothalamus and striatum in a rat model.

Upon ultrastructural examination, the morphology of mitochondria is a determinant of the pathophysiology of neurodegenerative diseases such as stroke. Ischemic damage induces changes in mitochondrial membrane permeability, followed by mitochondrial swelling and release of cytochrome c or other apoptosis-promoting factors into the cytoplasm [26]. Subsequently, release of these factors initiates an increase in the Bax to Bcl-2 ratio and activates caspase-3 [27]. Our results suggested that treatment with TMPP, BO, or the combination significantly attenuated the severity of abnormalities caused by ischemic injury, especially regarding the structure of mitochondria in neurons of hypothalamus and striatum. After GCIR injury, apoptosis plays a critical role in the molecular mechanism of cerebral dysfunction. In the present study, TUNEL assay was used to evaluate the level of neuronal apoptosis. The TMPP, BO, and combination therapy groups showed significant reductions in numbers of apoptotic neurons and AI compared to the model group. In addition, the improvement observed in the TMPP + BO group was greater than in either of the TMPP or BO monotherapy groups.

Numerous studies have indicated that caspase-3, Bcl-2 family, and p53 play crucial roles in neuron apoptosis after activation by a series of signal transduction reactions. In terms of function, Bcl-2 family members can be divided into two groups, pro-apoptotic members includ-

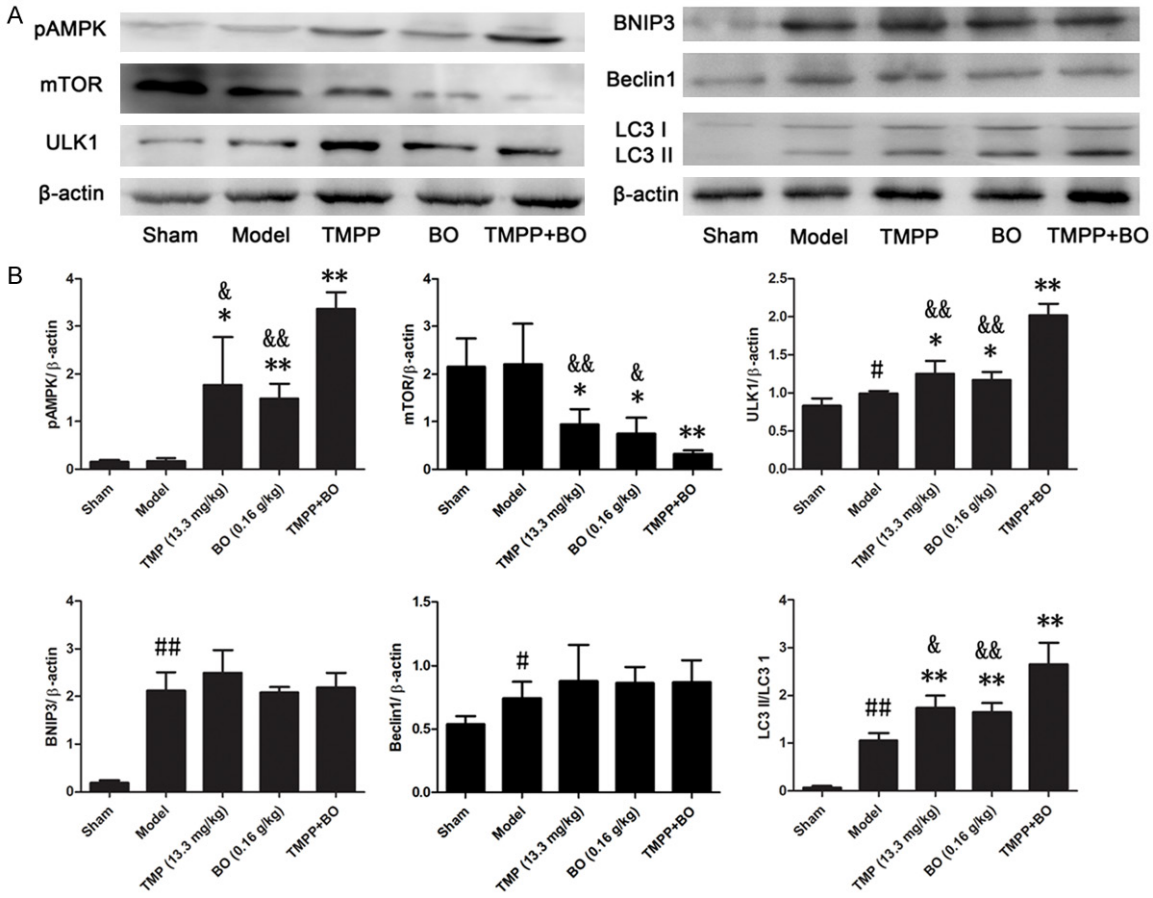

Figure 6. The cooperative effect between TMPP and BO on regulating the expression of autophagy-related proteins in hypothalamus of GCIR rats. A. Western blot results for p-AMPA, mTOR, ULK1, BNIP3, Beclin1, and LC3 II/I. B. Column charts of the expression of these proteins in each group. *n*=4. The results suggested that treatment with TMPP, BO, or the combination, regulated autophagy by increasing expression of pAMPK, ULK1, and LC3 II/I, and decreasing expression of mTOR in ischemic hypothalamus. The effect of the combination therapy was greater than either monotherapy.

ing Bax and Bid, and anti-apoptotic members including Bcl-2 and Bcl-X_L. The transcription factor p53, regarded as the first decision factor in the apoptosis cascade, controls the expression of many apoptosis-related genes. Kiraz reported that p53 induced the expression of several proteins, such as Bax and Bid, through a transcription-dependent apoptotic pathway [28]. Therefore, the expression of p53 and its related genes plays a crucial role in neuronal apoptosis that results from ischemic injury. In the present study, treatment of rats with TMPP, BO, or the combination significantly reduced the transcription levels of p53 and caspase-3 in neurons from the two brain regions. Both TMPP and the combination therapy markedly increased Bcl-2 and decreased Bax expression. The combination therapy reduced the expression of these apoptosis-related genes more strongly than the TMPP and BO monotherapies.

Autophagy is a highly controlled lysosome-mediated activity in eukaryotes that eliminates damaged, aged, or long-lived proteins and organelles like ER and mitochondria. Autophagy produces amino acids and free fatty acids that can be used to synthetize new adenosine triphosphate (ATP) and protein, and ultimately maintains cellular survival [29]. The formation of the autophagosome, a double membrane vesicle that sequesters part of the cytoplasm and fuses with lysosomes, is the common marker of autophagy activity [30]. It has been confirmed that modulation of the expression of pAMPK, mTOR, BNIP3, Beclin1, LC3 II/I, and ULK1 can affect the autophagy signaling net-

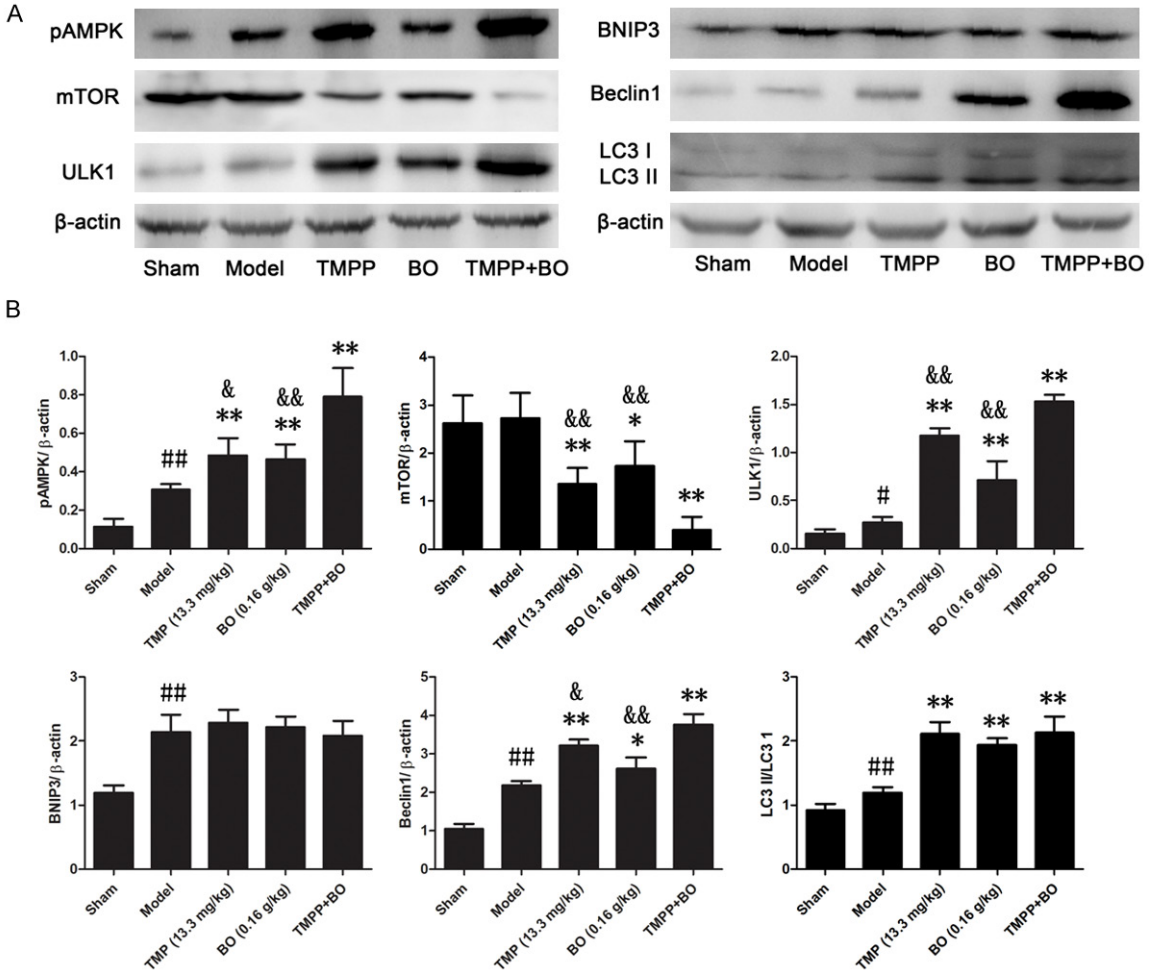

Figure 7. The cooperative effect between TMPP and BO on regulating the expression of autophagy-related proteins in striatum of GCIR rats. A. Western blot results for p-AMPA, mTOR, ULK1, BNIP3, Beclin1, and LC3 II/I. B. Column charts of the expression of these proteins in each group. *n*=4. The results suggested that treatment with TMPP, BO, or the combination regulated autophagy by increasing expression of pAMPK, ULK1, Beclin1, and LC3 II/I, and decreasing expression of mTOR in ischemic striatum. The effect of the combination therapy was greater than either monotherapy.

work in ischemic neurons [31, 32]. As shown in **Figure 9**, ROS and hypoxia are the main triggers of autophagy. ROS stimulates the formation of pAMPK, which inhibits the expression of mTOR [33]. Inhibition of mTOR reversely promotes ULK1 expression, and induces the transformation of LC3 I to LC3 II. The increase of LC3 II/LC3 I contributes to formation of the autophagosome [34]. Hypoxia has two pathways to trigger autophagy. One is similar to ROS via the pAMPK-mTOR-ULK1 pathway. The other is the BNIP3-Beclin1 signaling pathway. After up-regulation of Beclin1 following the increase of BNIP3, the ratio of LC3 II to LC3I is elevated, which indicates the formation of the final autophagy marker [35]. In our study, damage from brain ischemia slightly initiated the autophagy cascade, which was similar to previous reports [36]. Interestingly, autophagy was not down-regulated, but further up-regulated after the rats were treated with TMPP, BO, and the combination, and the different treatments resulted in different effects in the two brain regions. In hypothalamus, it was speculated that treatment with TMPP, BO, or the combination promoted autophagy via increased AMPK phosphorylation, suppressed mTOR activation, and enhanced ULK1 expression. In striatum, in addition to regulation of the pAMPK–mTOR–ULK1 pathway as in hypothalamus, the treatments promoted autophagy by activating Beclin1 expression. Furthermore, the combina-

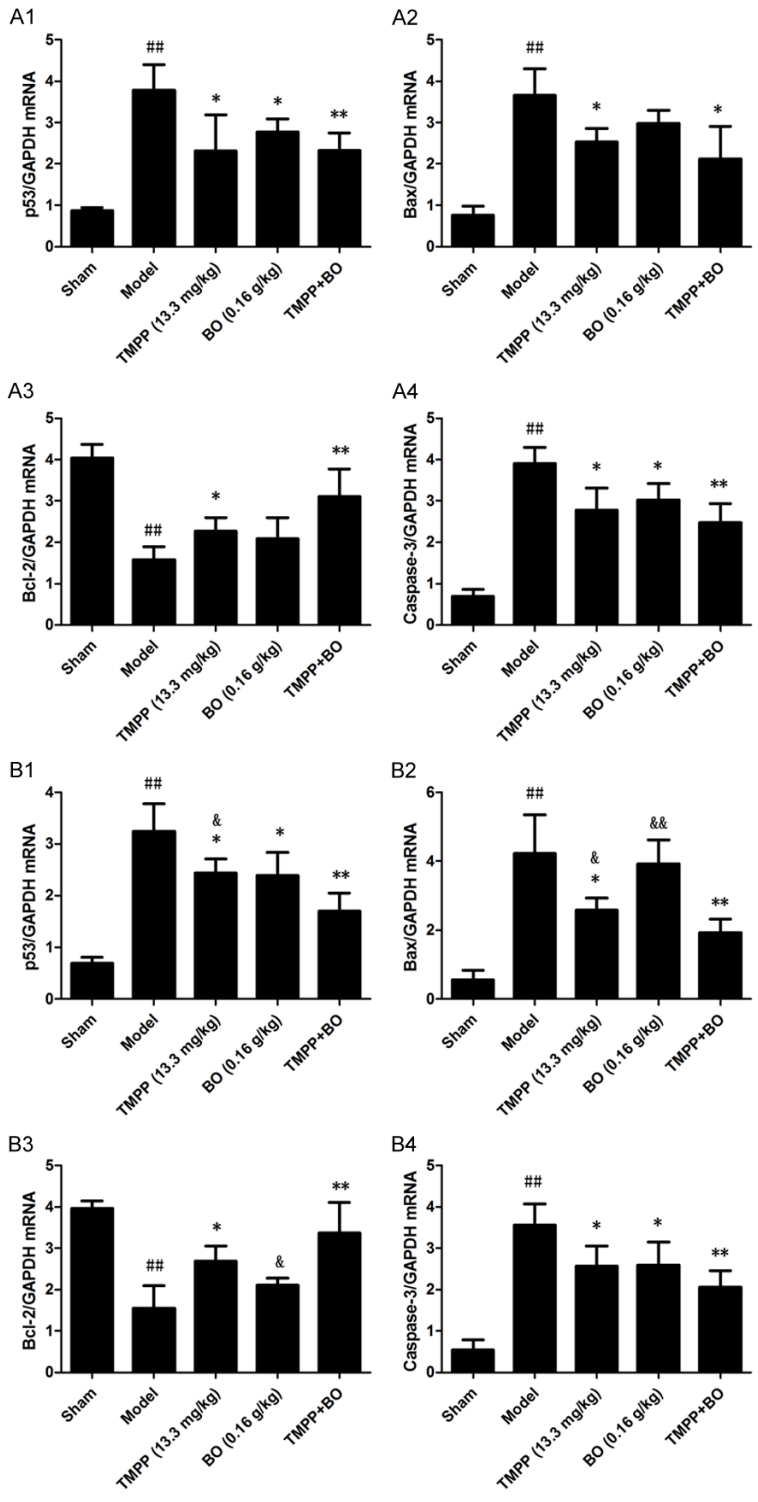

Figure 8. The cooperative effect between TMPP and BO on regulating the expression of apoptosis-related genes in hypothalamus and striatum of GCIR rats (n=4). A represents hypothalamus, and B represents striatum. The results suggested that TMPP regulated apoptosis by reducing the expression of p53 and caspase-3 and the Bax/Bcl-2 ratio, and while BO reduced expression of p53 and caspase-3 in the two brain regions. The effect of the combination therapy was greater than either monotherapy.

tion therapy exhibited a greater ability to promote autophagy than TMPP or BO monotherapy.

Autophagy and apoptosis are two different modes of cell death. Therefore, what factor (s) may decide the definitive manner of neuronal death? Interestingly, a recent study reported that elevation of $[Ca^{2+}]i$ might be the switch that shifts cells from autophagy to apoptosis [37]. Similarly, Li further confirmed that enhancement of $[Ca^{2+}]i$ shifted the cell from autophagy to apoptosis in an H. armigera epidermal cell line [38]. In the present study, treatment with TMPP, BO, or the combination attenuated the Ca^{2+} overload in both cerebral regions after ischemia-reperfusion damage. Compared to TMPP or BO monotherapy, the combined therapy group exhibited a greater reduction in $[Ca^{2+}]i$. Thus, our study confirmed that TMPP + BO combination therapy might have the ability to shift neurons from apoptosis to autophagy via modulating neuronal $[Ca^{2+}]i$, and that its synergistic effect was greater than either of the monotherapies.

Conclusion

The present study demonstrated the synergistic effects between TMPP and BO for treating ischemia-reperfusion injury in hypothalamus and striatum of rats. The potential mechanisms involved shifting of neurons from harmful apoptosis to protective autophagy. Moreover, the shift might be related to the reduction of neuronal $[Ca^{2+}]i$.

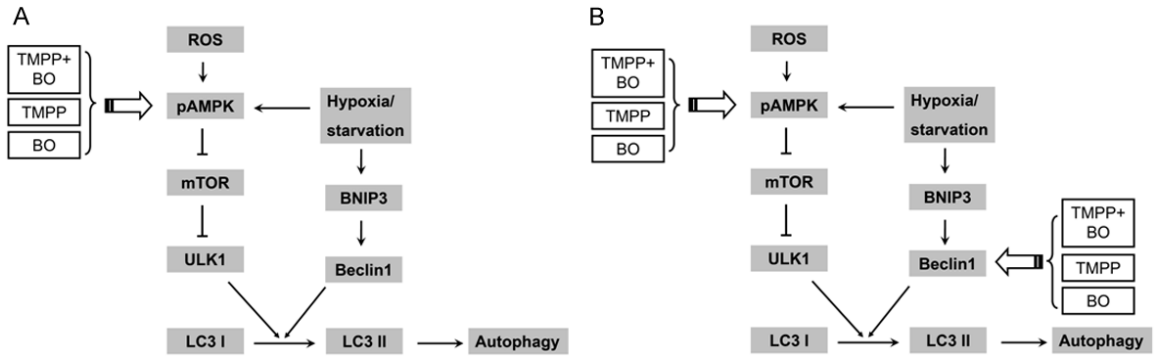

Figure 9. The pAMPK-mTOR-ULK1/BNIP3-Beclin1 autophagy signaling pathways and the synergistic effects TMPP and BO on those pathways. (A) Represents hypothalamus and (B) represents striatum. It was suggested that TMPP, BO, and the combination therapy might have the same target in autophagy modulation. In hypothalamus, the target might be pAMPK while in striatum, the target might be both pAMPK and Beclin1.

Acknowledgements

This study was supported by the National Natural Science Foundation of China (81573713, 81403079, 81560588, 81673566, 81573556), Basic Research Project (Natural Science Foundation) of Jiangsu Province (BK20151564, BK20150088, BK20141467), the Priority Academic Program Development of Jiangsu Higher Education Institutions (PAPD), the Qinglan Project of Jiangsu Province, the Innovated Team of the Education Department of Guizhou Province (2014-31), the Scientific and Technologic Innovated Team of Guizhou Province (2015-4025), the High level Innovation Talents (2015-4029), Jiangsu Provincial Key Construction Laboratory (No. SuJiaoKe[2016]8), the Guizhou Provincial Key Technology R&D Program (NO. 2016-2826).

Disclosure of conflict of interest

None.

Address correspondence to: Hai-Bo Cheng, Jiangsu Engineering Laboratory for Research and Industrialization of Empirical Formulae, Nanjing University of Chinese Medicine, Nanjing 210023, China. E-mail: hb_chen1900@163.com; Xiang-Chun Shen, The Key Laboratory of Optimal Utilization of Natural Medicinal Resources, School of Pharmaceutic Science, Guizhou Medical University, Huaxi University Town, Guian New District, Guiyang 550025, China. E-mail: shenxiangchun@126.com

References

[1] Chauhan NR, Kapoor M, Prabha Singh L, Gupta RK, Chand Meena R, Tulsawani R, Nanda S and Bala Singh S. Heat stress-induced neuroinflammation and aberration in monoamine levels in hypothalamus are associated with temperature dysregulation. Neuroscience 2017; 358: 79-92.

[2] Mohammadi MT. Overproduction of nitric oxide intensifies brain infarction and cerebrovascular damage through reduction of claudin-5 and ZO-1 expression in striatum of ischemic brain. Pathol Res Pract 2016; 212: 959-964.

[3] Tai PA, Chang CK, Niu KC, Lin MT, Chiu WT and Lin JW. Reduction of ischemic and oxidative damage to the hypothalamus by hyperbaric oxygen in heatstroke mice. J Biomed Biotechnol 2010; 2010: 609526.

[4] Ya BL, Li HF, Wang HY, Wu F, Xin Q, Cheng HJ, Li WJ, Lin N, Ba ZH, Zhang RJ, Liu Q, Li YN, Bai B and Ge F. 5-HMF attenuates striatum oxidative damage via Nrf2/ARE signaling pathway following transient global cerebral ischemia. Cell Stress Chaperones 2017; 22: 55-65.

[5] Nakashima MN, Yamashita K, Kataoka Y, Yamashita YS and Niwa M. Time course of nitric oxide synthase activity in neuronal, glial, and endothelial cells of rat striatum following focal cerebral ischemia. Cell Mol Neurobiol 1995; 15: 341-349.

[6] Zirh TA, Iskender E, Onat F, Pamir MN and Oktay S. Muscarinic receptors in rat cortex, hippocampus, hypothalamus and brainstem following transient forebrain ischemia and hemorrhagic shock. Neurosci Lett 1994; 181: 13-16.

[7] Zhang Y, Lan R, Wang J, Li XY, Zhu DN, Ma YZ, Wu JT and Liu ZH. Acupuncture reduced apoptosis and up-regulated BDNF and GDNF expression in hippocampus following hypoxia-ischemia in neonatal rats. J Ethnopharmacol 2015; 172: 124-132.

[8] Wang Y, Han R, Liang ZQ, Wu JC, Zhang XD, Gu ZL and Qin ZH. An autophagic mechanism is

involved in apoptotic death of rat striatal neurons induced by the non-N-methyl-D-aspartate receptor agonist kainic acid. Autophagy 2008; 4: 214-226.
[9] Sun Y, Jiang J, Zhang Z, Yu P, Wang L, Xu C, Liu W and Wang Y. Antioxidative and thrombolytic TMP nitrone for treatment of ischemic stroke. Bioorg Med Chem 2008; 16: 8868-8874.
[10] Chang CY, Kao TK, Chen WY, Ou YC, Li JR, Liao SL, Raung SL and Chen CJ. Tetramethylpyrazine inhibits neutrophil activation following permanent cerebral ischemia in rats. Biochem Biophys Res Commun 2015; 463: 421-427.
[11] Kao TK, Ou YC, Kuo JS, Chen WY, Liao SL, Wu CW, Chen CJ, Ling NN, Zhang YH and Peng WH. Neuroprotection by tetramethylpyrazine against ischemic brain injury in rats. Neurochem Int 2006; 48: 166-176.
[12] Tang Q, Han R, Xiao H, Shen J, Luo Q and Li J. Neuroprotective effects of tanshinone IIA and/or tetramethylpyrazine in cerebral ischemic injury in vivo and in vitro. Brain Res 2012; 1488: 81-91.
[13] Chen XH, Lin ZZ, Liu AM, Ye JT, Luo Y, Luo YY, Mao XX, Liu PQ and Pi RB. The orally combined neuroprotective effects of sodium ferulate and borneol against transient global ischaemia in C57 BL/6J mice. J Pharm Pharmacol 2010; 62: 915-923.
[14] Yu B, Ruan M, Cui XB, Guo JM, Xu L and Dong XP. Effects of borneol on the pharmacokinetics of geniposide in cortex, hippocampus, hypothalamus and striatum of conscious rat by simultaneous brain microdialysis coupled with UPLC-MS. J Pharm Biomed Anal 2013; 77: 128-132.
[15] Yu B, Ruan M, Sun Y, Cui X, Yu Y, Wang L and Fang T. Effect of borneol and electroacupuncture on the distribution of hyperforin in the rat brain. Neural Regeneration Research 2011; 6: 1876-1882.
[16] Kong QX, Wu ZY, Chu X, Liang RQ, Xia M and Li L. Study on the anti-cerebral ischemia effect of borneol and its mechanism. Afr J Tradit Complement Altern Med 2014; 11: 161-164.
[17] Liu R, Zhang L, Lan X, Li L, Zhang TT, Sun JH and Du GH. Protection by borneol on cortical neurons against oxygen-glucose deprivation/reperfusion: involvement of anti-oxidation and anti-inflammation through nuclear transcription factor kappaappaB signaling pathway. Neuroscience 2011; 176: 408-419.
[18] Wu HY, Tang Y, Gao LY, Sun WX, Hua Y, Yang SB, Zhang ZP, Liao GY, Zhou QG, Luo CX and Zhu DY. The synergetic effect of edaravone and borneol in the rat model of ischemic stroke. Eur J Pharmacol 2014; 740: 522-531.
[19] Huang P, H. WQ, Rong XL, Lei WW, Bei ML, Han J and Wu LN. Protective effects of borneolum combined with rhizoma chuanxiong on cerebral ischemia withi reperfusion injury. J Guangzhou Univ Tradit Chin Med 2000; 323-326.
[20] Huang P, Wu QH, Rong XL and Han J. Mechanismof borneolum combined with rhizoma chuanxiong in counteracting cerebral ischemia with reperfusion injury. J Guangzhou Univ Tradit Chin Med 2001; 332-334.
[21] Wang H. Enhancement of synthetic borneol on ligustrazine resisting aoute hypoxia in mice. Pharmaco Clin Chin Materia Medica 2000; 16: 13-15.
[22] Xu HC. Xiongbing nasal spray for vertebral and basilar arterial insufficiency. Chin J Integr Med Cardio-/Cerebrovasc Dis 2006; 4: 388-390.
[23] Yu B, Ruan M, Zhang ZN, Cheng HB and Shen XC. Synergic effect of borneol and ligustrazine on the neuroprotection in global cerebral ischemia/reperfusion Injury: a region-specificity study. Evid Based Complement Alternat Med 2016; 2016: 4072809.
[24] Curras-Collazo MC, Patel UB and Hussein MO. Reduced susceptibility of magnocellular neuroendocrine nuclei of the rat hypothalamus to transient focal ischemia produced by middle cerebral artery occlusion. Exp Neurol 2002; 178: 268-279.
[25] Chen SH, Lin MT and Chang CP. Ischemic and oxidative damage to the hypothalamus may be responsible for heat stroke. Curr Neuropharmacol 2013; 11: 129-140.
[26] Mullauer FB, Kessler JH and Medema JP. Betulinic acid induces cytochrome c release and apoptosis in a Bax/Bak-independent, permeability transition pore dependent fashion. Apoptosis 2009; 14: 191-202.
[27] Nam YJ, Kim A, Lee MS, Shin YK, Sohn DS and Lee CS. Lamotrigine attenuates proteasome inhibition-induced apoptosis by suppressing the activation of the mitochondrial pathway and the Caspase-8- and Bid-Dependent pathways. Neurochem Res 2016; 41: 2503-2516.
[28] Kiraz Y, Adan A, Kartal Yandim M and Baran Y. Major apoptotic mechanisms and genes involved in apoptosis. Tumour Biol 2016; 37: 8471-8486.
[29] Levine B and Klionsky DJ. Development by self-digestion: molecular mechanisms and biological functions of autophagy. Dev Cell 2004; 6: 463-477.
[30] Heras-Sandoval D, Perez-Rojas JM, Hernandez-Damian J and Pedraza-Chaverri J. The role of PI3K/AKT/mTOR pathway in the modulation of autophagy and the clearance of protein aggregates in neurodegeneration. Cell Signal 2014; 26: 2694-2701.
[31] Alers S, Loffler AS, Wesselborg S and Stork B. Role of AMPK-mTOR-Ulk1/2 in the regulation of autophagy: cross talk, shortcuts, and feedbacks. Mol Cell Biol 2012; 32: 2-11.

[32] Levine B and Yuan J. Autophagy in cell death: an innocent convict? J Clin Invest 2005; 115: 2679-2688.
[33] Meley D, Bauvy C, Houben-Weerts JH, Dubbelhuis PF, Helmond MT, Codogno P and Meijer AJ. AMP-activated protein kinase and the regulation of autophagic proteolysis. J Biol Chem 2006; 281: 34870-34879.
[34] Park KK, Liu K, Hu Y, Kanter JL and He Z. PTEN/mTOR and axon regeneration. Exp Neurol 2010; 223: 45-50.
[35] Liang XH, Jackson S, Seaman M, Brown K, Kempkes B, Hibshoosh H and Levine B. Induction of autophagy and inhibition of tumorigenesis by beclin 1. Nature 1999; 402: 672-676.
[36] Wang PR, Wang JS, Zhang C, Song XF, Tian N and Kong LY. Huang-Lian-Jie-Du-Decotion induced protective autophagy against the injury of cerebral ischemia/reperfusion via MAPK-mTOR signaling pathway. J Ethnopharmacol 2013; 149: 270-280.
[37] Borodkina AV, Shatrova AN, Deryabin PI, Griukova AA, Abushik PA, Antonov SM, Nikolsky NN and Burova EB. Calcium alterations signal either to senescence or to autophagy induction in stem cells upon oxidative stress. Aging (Albany NY) 2016; 8: 3400-3418.
[38] Li YB, Li XR, Yang T, Wang JX and Zhao XF. The steroid hormone 20-hydroxyecdysone promotes switching from autophagy to apoptosis by increasing intracellular calcium levels. Insect Biochem Mol Biol 2016; 79: 73-86.